Journal of Particle Science and Technology *11* (2) (2025) 93-100

Iranian Research Organization for Science and Technology (IROST)

Journal of PARTICLE Science & Technology

JPSIT
https://jpst.irost.ir
Online ISSN: 2423-4079
Print ISSN: 2423-4087

Effect of Zr particles and RRA heat treatment on grain boundary precipitation of 7055 aluminum alloys

Mehdi Shakoory, Mohammad Esmailian✉, Morteza Taheri

Department of Advanced Materials and New Technology, Iranian Research Organization for Science and Technology (IROST), Tehran, Iran

HIGHLIGHTS

- Retrogression and re-aging (RRA) heat treatment improves both the mechanical strength and the stress-corrosion resistance of the 7055 aluminum alloy.
- After RRA heat treatment, better distribution and composition changes of the precipitates have been achieved.
- With the addition of Zr, this element remains within the grains during heat treatment and inhibits grain growth, thereby improving the mechanical properties and corrosion resistance of the aluminum alloy.

GRAPHICAL ABSTRACT

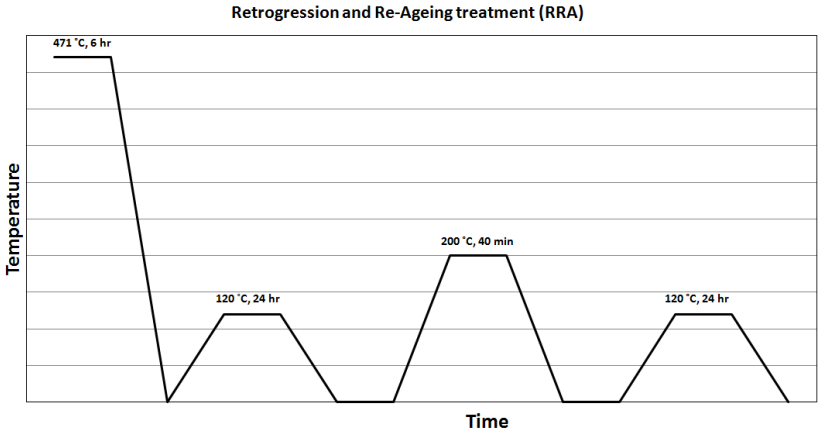

ARTICLE INFO

Article type:
Research article

Article history:
Received 16 November 2025
Received in revised form 09 February 2026
Accepted 14 February 2026

Keywords:
7055 Al Treatment
Zr in Al Grain boundary
Al 7055 Corrosion
Zr in Al 7055

ABSTRACT

Due to its high strength and corrosion resistance, aluminum alloy 7055 is widely used in aerospace structures. However, its susceptibility to stress corrosion cracking (SCC) limits its performance. In this study, the combined effects of zirconium (Zr) addition and retrogression and re-aging (RRA) heat treatment on the microstructure, grain boundary precipitates, and stress corrosion resistance (SCR) of 7055 aluminum alloy were investigated. For property evaluation, microstructural characterization was carried out using scanning electron microscopy (SEM) and energy dispersive X-ray spectroscopy (EDS), while mechanical and stress corrosion tests were conducted according to ASTM standards. The results showed that Zr addition refined the grains and promoted the formation of Al_3Zr particles within the matrix, inhibiting grain growth during heat treatment. RRA treatment accompanied by Zr addition improved the mechanical strength from 528 to 608 MPa and increased the stress corrosion resistance from 68 to 96 %. The combined effect of Zr addition and RRA treatment resulted in a more stable microstructure, with improved strength and resistance to stress-corrosion cracking.

DOI: 10.22104/jpst.2026.7865.1287

✉ *Corresponding author: E-mail address:* m.esmailian555@gmail.com; *Tel:* +9821-57416242

1. Introduction

Al–Zn–Mg–Cu alloys, AA7055 series, are disposed to severe localized corrosion, such as intergranular corrosion [1]. The low resistance to localized corrosion presents a difficulty for the application of Al–Zn–Mg–Cu alloys in the aerospace industry. A heat treatment operation rearranges the microstructure of the alloy in order to produce the best mechanical properties and stress corrosion resistance [2].

Commercial T6[1] treatment can improve the strength, but it decreases the stress corrosion resistance [3]. Overaging treatment, such as T73[2], improves the stress corrosion resistance of aluminum alloys [4], but to simultaneously achieve a good stress corrosion resistance and strength, a retrogression and re-ageing (RRA) treatment is recommended [5]. The RRA temper is a T6 temper, which is then followed by a short time retrogression at a higher temperature, quenching in water or cooling air, followed by a reaging treatment similar to the T6 temper. Changes in precipitate microstructures during retrogression and reaging treatments have been reported by several studies [6,7]. Investigations show that fine $\acute{\eta}$ precipitates inside the aluminum grains and some GP[3] zones partially dissolve during retrogression and reprecipitate during the reaging process [8]. Finally, the η phase precipitates and grows in the grain boundaries [7]. Jun-chao *et al.* investigated the effect of Zr on mechanical properties and found that with Zr addition, significant improvements in the mechanical properties of the annealed alloys could be obtained [8]. Corrosion testing results show that, with Zr addition, the corrosion resistance of the as-annealed alloy decreases.

Liu *et al.* found that Zr inhibited recrystallization and refined grain size, which in turn allowed subgrain boundaries to retard the propagation of the track and improve corrosion resistance [9]. Meanwhile, other researchers found that by vibrating the alloy, the grain boundary precipitates (GBPs) change from continuous to discontinuous, producing the proper width of the precipitate-free zone (PFZ), which increases the electrical conductivity and corrosion resistance [10]. Men-Zhen *et al.* added Yb/Zr particles into an Al series 7000 alloy and found that grain refinement treatment has a severe effect on the increase of both strength and elongation [11]. They found that grain refiningincreased the ultimate tensile strength up to 705.3 MPa, and elongation up to 8.7 %, with Yb/Zr modification. Moreover, by adding Yb/Zr, the distribution of $MgZn_2$ phases along grain boundaries became more discontinuous in the alloy, which prevented the propagation of intergranular corrosion and improving the corrosion resistance.

In recent years, increasing attention has been paid to optimizing the combined mechanical and corrosion performance of 7xxx aluminum alloys through advanced heat treatments and microalloying strategies. Ren *et al.* systematically investigated the RRA treatment of AA7055 [12]. They reported that an optimized retrogression temperature effectively modified grain boundary precipitates from continuous to semi-discontinuous morphologies, leading to a significant improvement in stress corrosion cracking resistance while retaining high strength. Meanwhile, Jiang *et al.* demonstrated that minor Zr addition promoted the formation of fine Al_3Zr dispersoids, which effectively inhibited recrystallization and stabilized subgrain structures during subsequent heat treatments, resulting in enhanced corrosion resistance and mechanical stability [13]. More recently, Liu *et al.* studied the synergistic effect of RRA treatment and Zr microalloying in 7xxx alloys and found that Zr-containing alloys exhibited a narrower and more uniform precipitate-free zone (PFZ) after RRA, which played a critical role in suppressing intergranular corrosion propagation [14]. In addition, Rodinger *et al.* reported that the presence of Zr improved the thermal stability of η' precipitates during retrogression, contributing to a better balance between strength and corrosion resistance compared with conventional RRA-treated alloys without Zr [15].

In this study, the combined effects of Zr addition and retrogression and re-aging (RRA) heat treatment on the microstructure and stress corrosion behavior of 7055 aluminum alloy were systematically investigated. While previous studies have mainly focused on either Zr modification or RRA treatment alone, the present work aims to reveal the synergistic influence of Zr and RRA on grain boundary precipitation, phase composition, and stress corrosion resistance. This integrated approach provides new insight into the optimization of both mechanical strength and corrosion resistance in high-strength 7000-series aluminum alloys.

2. Materials and methods

2.1. Materials

The aluminum material in this study was selected as 6 mm thick sheets. To prepare the sheets, they were first melted, and then alloyed, cast, homogenized, hot rolled, and heat treated.

---

[1] The T6 temper involves solution treatment, quenching, and low-temperature aging, producing fine η' precipitates and Guinier-Preston (GP) zones responsible for peak strength.

[2] The T73 temper represents an overaged condition obtained by extended aging at higher temperatures, forming coarser and more stable precipitates with improved stress-corrosion resistance.

[3] GP zones are nanoscale clusters of solute atoms (Zn–Mg) that act as precursors for η'/η phases during artificial aging.

The chemical composition of the alloy was the commercially available 7055 alloy (Table 1).

An amount of 0.3 wt% Zr was added to the alloy after the melting for control of grain growth during heat treatment and solutionizing operations. For alloying preparation, an induction melting furnace with a 5 kg melting capacity was used.

Table 1. Chemical composition (wt%) of the base 7055 aluminum alloy.

Zn	Mg	Cu	Zr	Fe	Si	Mn	Cr	Ti	Al
7.6	2.0	1.6	0.08	0.10	0.05	0.05	0.04	0.03	Bal.

2.2. Sample preparation

For sample making, the molten metal was cast in a water-cooled copper mould. After moulding, the as-cast specimens were homogenized at 490 ºC for 24 h and then hot rolled to about 35 % reduction. Hot rolling was performed by a lab rolling mill with a 50 rpm rolling speed at 440 ºC. The samples were then cut into tensile size according to ASTM E8M standard [16]. After cutting and preparing the samples, solution heat treatment was applied at 471 ºC for 6 h, and then the samples were quenched in water. The 6 percent predeformation was applied to samples before the next heat treatment, and then artificial aging at 120 ºC for 24 h was performed (T6 temper). After this operation, the RRA heat treatment was applied to the samples. The retrogression stage was carried out in a preheated air-circulation furnace at a precise temperature of 200 ± 2 °C for a duration of 40 min. Following this, the samples were rapidly water-quenched (quenching rate > 100 °C.s^{-1}) to room temperature to retain the solute distribution achieved during retrogression. Finally, the samples underwent re-aging in an oil bath at 120 ± 1 °C for 24 h to complete the RRA cycle. The schematic of this process is shown in Fig. 1.

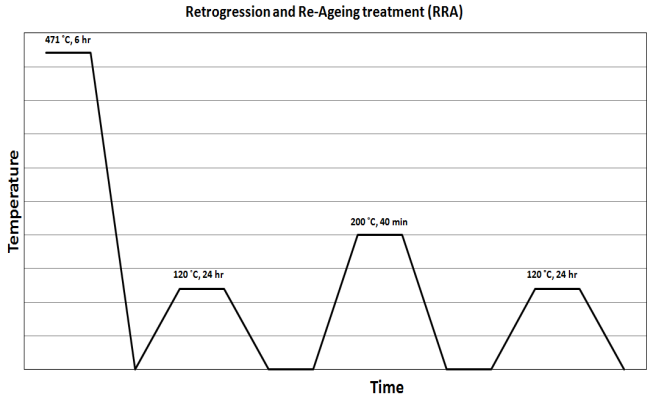

Fig. 1. Scheme of the RRA heat treatment procedure.

2.3. Testing instruments

All mechanical testing was performed at ambient temperature according to the ASTM B557-06 small size standard test with a strain rate of 4 to 10 s^{-1}. Three parallel specimens were prepared and tested for each heat treatment condition (T6 and RRA with Zr addition), to ensure reproducibility. The reported values of ultimate tensile strength (UTS) and stress corrosion resistance represent the average of three independent measurements, and the error bars in the figures and tables correspond to one standard deviation from the mean.

The SEM analysis was performed using a TESCAN scanning electron microscope. An SEM equipped with an EDS was used to characterize the second-phase precipitations in alloys.

The stress corrosion tests were performed according to ASTM G139 standard [17]. A neutral 3.5 % sodium chloride solution was prepared and used according to ASTM G44 standard [18]. ASTM G49 standard [19] was used for sample preparation of the direct tension stress corrosion test. Briefly, a constant 207 MPa stress was first applied to the samples, and then a 4-day cycle time was used according to section 8-2 of the ASTM G139 standard. To eliminate the corrosion effects, other than SCC (such as pitting), some specimens were placed in a corrosion solution without stressing.

3. Results and discussion

The remaining strength for stressed samples compared to unstressed samples by percent, which is the SCC factor, is shown in Table 2 for different alloys.

As can be seen, RRA heat treatment increases the mechanical strength from 528 to 608 MPa. After the reversion stage, unstable and metastable precipitates dissolve in the aluminum matrix and form a solid solution for re-aging. Dissolved elements in the matrix will precipitate as fine and more distributed particles after re-aging and prevent dislocation movement, which results in increasing the mechanical strength. Fig. 2 shows a comparison between the precipitate distributions of particles in the matrix after Zr addition, RRA, and T6 heat treatments.

Table 2 shows the test results and SCR criteria. It can be concluded that the stress corrosion resistance of each alloy with different tempers can be easily calculated and compared with each other. Table 2 shows that the stress corrosion resistance increased after RRA heat treatment and Zr addition. After T6 heat treatment, the SCR is 68 %, but after Zr addition and RRA heat treatment, it increases to 96 %. This means that 96 % of the strength in 7055 alloys is retained after RRA heat treatment and Zr addition.

Table 2. Mechanical strength and stress corrosion test of 7055 alloy.

Temper	UTS-MPa (A)	UTS after 4 days without stress MPa (B)	UTS after 4 days with 207 MPa stress (MPa) (C)	Remaining strength after 4 days without stress (%) (D = B/A)	Remaining strength after 4 days with 207 MPa stress (%) (E= C/A)	Stress corrosion resistance (%) (E/D)
T6	528 ± 1.8	490 ± 1.4	333 ± 0.9	92.8 ± 0.7	63.1 ± 0.2	68 ± 1
RRA	608 ± 2.1	557 ± 2	534 ± 1.5	91.6 ± 0.8	87.8 ± 0.5	96 ± 0.8

A more detailed comparison of Fig. 2 reveals that the precipitate morphology and distribution are strongly dependent on the applied heat treatment. In the T6 condition (Fig. 2(a)), the precipitates are relatively coarse, densely distributed along the grain boundaries, and partially continuous, which leads to severe micro-galvanic coupling and reduced stress-corrosion resistance. In contrast, after RRA treatment with Zr addition (Fig. 2(b)), the precipitates become finer and more uniformly dispersed within the matrix, while grain boundary precipitates exhibit a more discontinuous morphology. The presence of stable, nanoscale Al_3Zr dispersoids restricts grain growth and provides preferential nucleation sites, retarding precipitate coarsening.

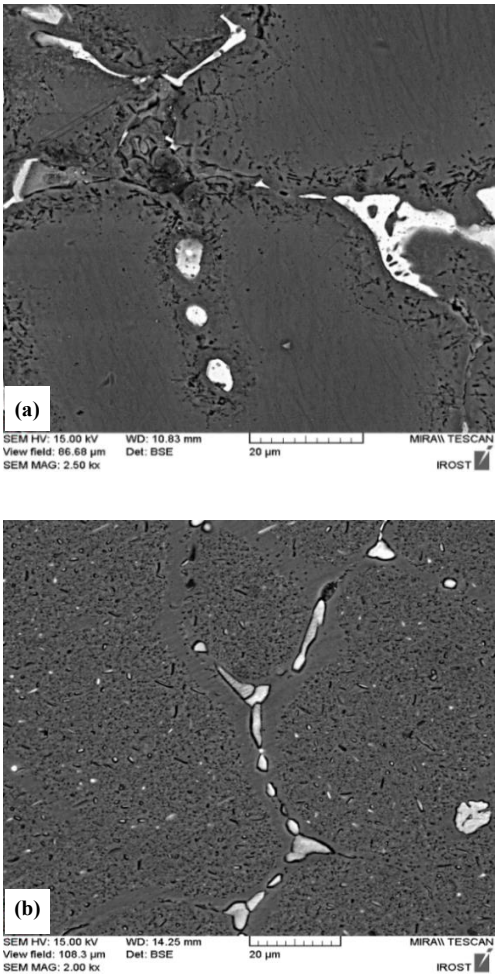

Fig. 2. SEM of 7055 alloy after (a) T6 and (b) RRA heat treatment and Zr addition.

This microstructural refinement enhances the Orowan strengthening mechanism and simultaneously reduces the potential difference between the matrix and grain boundary regions, thereby improving both tensile strength and corrosion resistance. The SEM micrographs in Fig. 2 provide critical insight into the microstructural mechanisms behind this performance enhancement. In the T6 condition (Fig. 2a), the coarse and semi-continuous network of grain boundary precipitates (GBPs) creates a preferential path for both crack propagation and anodic dissolution, explaining the lower SCR. Conversely, the RRA+Zr treatment (Fig. 2(b)) produces a refined and discontinuous distribution of GBPs. This morphological change is attributed to the partial dissolution of metastable phases during retrogression and the subsequent nucleation of finer, more stable precipitates during re-aging, aided by the grain-stabilizing effect of Al_3Zr dispersoids.The resulting microstructure effectively obstructs dislocation motion (enhancing strength) while breaking the continuity of corrosive pathways along boundaries (improving SCR).

Fig. 3 shows the EDS analyses of precipitates in the grain boundary after Zr addition, T6, and RRA heat treatment. As can be seen in Fig. 3, grain boundary precipitates have been enriched in copper after RRA heat treatment. Copper and zinc are the main alloying elements in 7055 aluminum alloy.

They have different diffusivity and atomic radius in the aluminum matrix; the atomic radius of Zn (≈ 0.134 nm) is slightly larger than that of Cu (≈ 0.128 nm), while the diffusivity of Zn atoms is about forty times higher than that of Cu atoms in aluminum alloys at approximately 150 °C [17]. Moreover, Zn atoms move faster and immigrate to grain boundary precipitates after one-step T6 heat treatment, so that grain boundary precipitates will be enriched with Zn atoms. During the reversion stage, the Zn atoms move faster than Cu and immigrate from the grain boundaries and dissolve in the aluminum matrix. After the re-aging heat treatment, Zn atoms will precipitate in the matrix, and more Cu atoms will remain in the grain boundary precipitates. Copper and zinc have opposite effects on the corrosion behavior of aluminum alloys [20,21]. Composition changes in precipitate composition, particularly depletion of Cu inside the grains and enrichment of grain boundaries from Cu after RRA treatment, lead to an increase in corrosion resistance of 7000 series aluminum alloy [22].

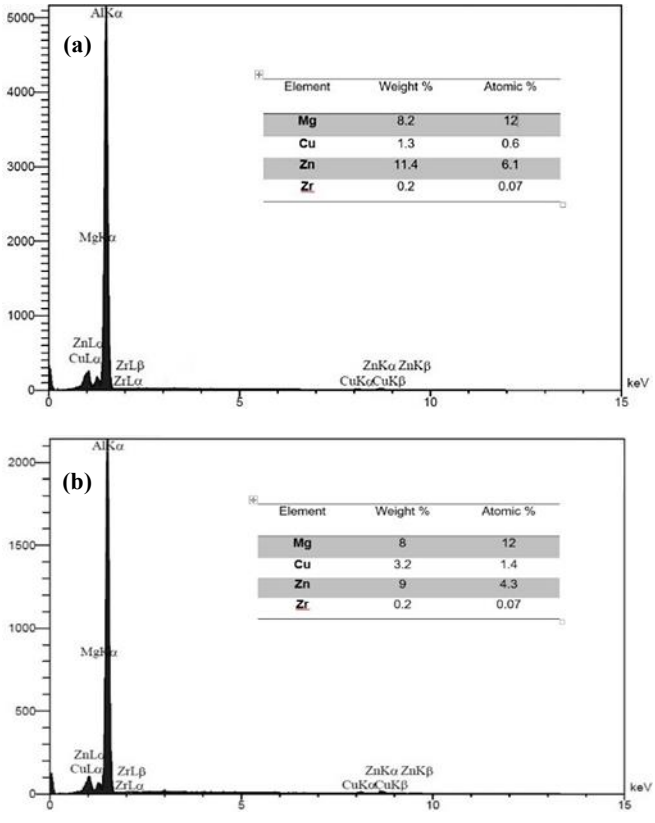

Fig. 3. Shows EDS analyses of grain 10precipitates after (a) T6 and (b) RRA heat treatment with Zr addition.

Moreover, as can be seen, there are no changes in the composition of Zr in the boundaries, which means that Zr can compose with Al to produce $ZrAl_3$ particles that remain inside the grains and prevent growth of grains, resulting in increases in mechanical properties and corrosion resistance of the aluminum alloy, and this is consistent with other researchers' works [23,24]. The EDS point analysis in Fig. 3 quantitatively corroborates the proposed elemental redistribution mechanism. The significant Cu enrichment at the grain boundary in the RRA-treated sample (Fig. 3(b)) compared to the T6 condition (Fig. 3(a)) is a direct consequence of the different diffusivities of Zn and Cu. During retrogression, the faster-diffusing Zn migrates back into the matrix, leaving behind Cu-rich precipitates at the boundaries. This Cu enrichment alters the electrochemical nature of the GBPs, reducing their anodic activity relative to the matrix and the adjacent precipitate-free zone (PFZ). This decreased potential gradient is a key factor in mitigating intergranular corrosion and stress corrosion cracking, as it lowers the driving force for galvanic attack. Fig. 4 illustrates the schematic ternary phase diagram of the Al–Cu–Zn system near the Al-rich corner. The diagram represents the primary solid-solution region of α-Al along with the two-phase areas ($\alpha + Al_2Cu$) and ($\alpha + MgZn_2$). The approximate composition of the commercial 7055 aluminum alloy (~ 7.6 wt% Zn, ~ 1.6 wt% Cu, balance Al) is marked by the red dot located inside the α-Al field. This location indicates that the alloy mainly exists as a supersaturated solid solution after quenching, from which strengthening precipitates ($\eta/MgZn_2$ and θ/Al_2Cu) evolve during aging. The proximity to the $\alpha + MgZn_2$ region confirms that Mg and Zn together dominate the precipitation sequence, while minor Cu enrichment contributes to secondary phase formation at grain boundaries.

Microstructural examinations revealed that the addition of zirconium markedly refined the grain structure, reducing the average grain size from approximately 80 µm to less than 30 µm (Fig. 5). This observation is consistent with previous reports [24]. The favorable properties achieved after heat treatment are directly correlated with this grain refinement. Since zirconium exhibits very limited solubility in aluminum, its addition promotes the formation of fine Al_3Zr dispersoids, as confirmed by several studies. These tetragonal equilibrium particles possess a lattice mismatch of less than 1 % with the aluminum matrix and typically form with dimensions below ~20 nm.

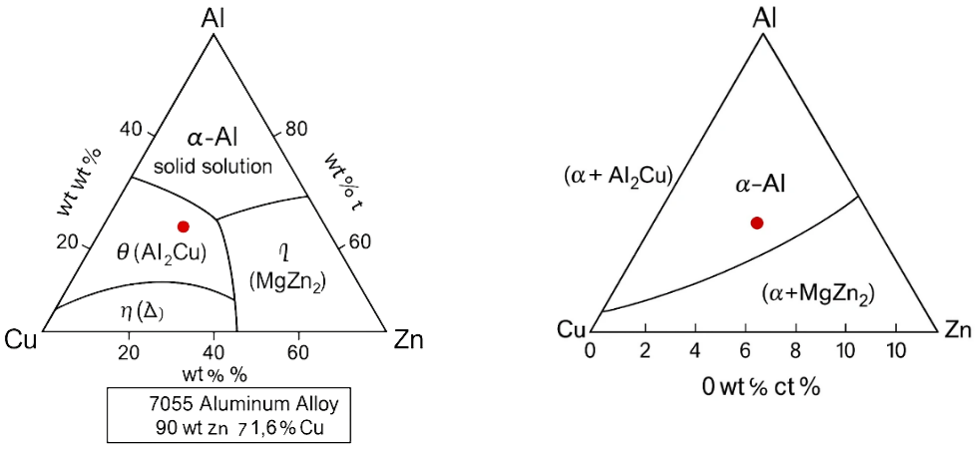

Fig. 4. Schematic ternary phase diagram of the Al–Cu–Zn system (Al-rich corner), showing major phase regions and the approximate composition of 7055 aluminum alloy indicated by the red dot.

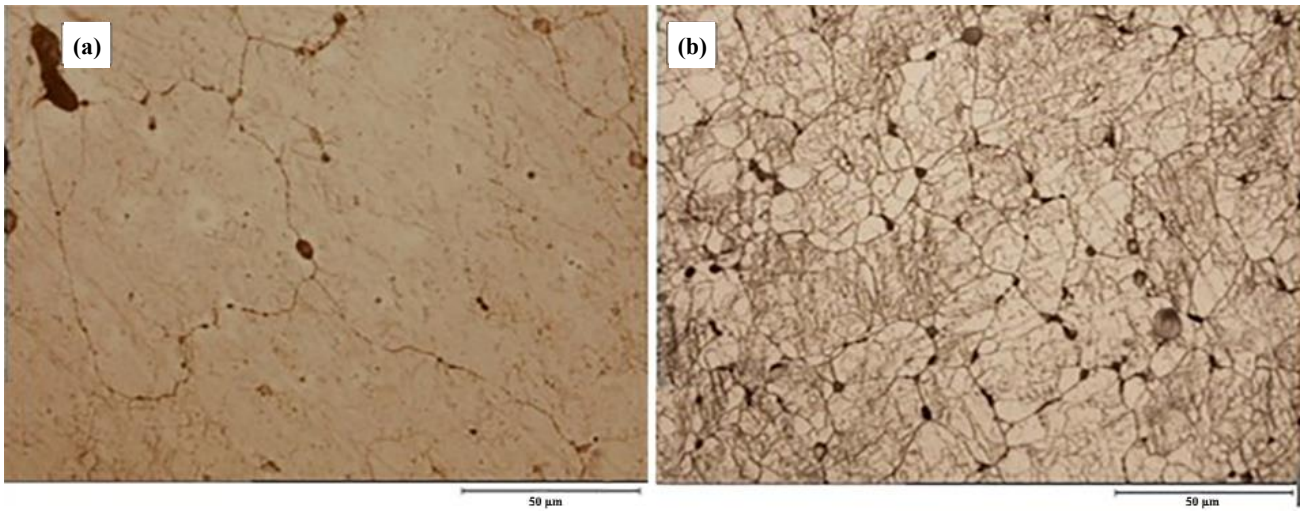

Fig. 5. Effect of zirconium on 7055 alloy after casting and T6 heat treatment: (a) Sample without zirconium; (b) Sample with 0.2 wt% zirconium. Fine-grain is evident in the sample containing zirconium (solution etching graph).

Owing to their coherent interface and thermal stability, these Al_3Zr dispersoids effectively inhibit grain growth during hot working and subsequent heat treatment, thereby contributing to improved strength and corrosion resistance [24].

To provide a deeper mechanistic understanding, it should be noted that the improvement in both strength and corrosion resistance during the RRA process is closely related to the evolution and redistribution of precipitates and the stabilizing role of Zr in the microstructure.

During the retrogression stage, partial dissolution of metastable η' and GP zones occurs, creating a supersaturated solid solution in the matrix. Subsequent re-aging enables the reprecipitation of a finer and more uniformly dispersed distribution of η' and η phases, which effectively impedes dislocation motion through the Orowan bypass mechanism, leading to the substantial increase in tensile strength.

Simultaneously, Zr atoms exhibit limited solid solubility and a very low diffusion coefficient in Al, resulting in the formation of stable Al_3Zr dispersoids. These fine coherent particles pin high-angle grain boundaries and inhibit recrystallization during both solution treatment and retrogression, thus maintaining a refined subgrain structure. This effect restricts the continuous precipitation of grain-boundary η-phase and promotes a discontinuous morphology with wider precipitate-free zones (PFZs), which are beneficial for stress corrosion resistance.

Moreover, the compositional change after RRA (Cu enrichment within grain-boundary precipitates and Zn enrichment within the matrix) reduces the electrochemical potential difference between the matrix and boundaries, thereby suppressing anodic dissolution pathways during exposure to chloride media. Consequently, the concurrent action of reprecipitation kinetics, boundary stabilization by Al_3Zr particles, and compositional homogenization accounts for the superior combination of strength and corrosion resistance observed in the Zr-modified 7055 alloy after RRA treatment.

4. Conclusion

This study aimed to clarify the combined effect of Zr addition and RRA heat treatment on the microstructure, grain boundary precipitation, and stress-corrosion behavior of high-strength 7055 aluminum alloy.

Through systematic mechanical testing and microstructural examination, the synergistic role of Zr and RRA was quantitatively evaluated.

1. RRA treatment significantly enhanced the alloy performance, raising the ultimate tensile strength from 528 to 608 MPa and increasing the stress-corrosion resistance from 68 to 96 %. These improvements are attributed to the dissolution and fine reprecipitation of η'/η phases during the retrogression and re-aging sequence.

2. Zirconium addition refined the grain structure, reducing average grain size from about 80 µm to below 30 µm through the formation of stable nanoscale Al_3Zr dispersoids (~20 nm), which effectively pinned grain boundaries and inhibited recrystallization and grain growth during heat treatment.

3. Microstructural analysis revealed that grain-boundary precipitates transformed from coarse, continuous networks (T6 condition) to finer, discontinuous morphologies after RRA+Zr treatment. This discontinuity widened precipitate-free zones and minimized galvanic coupling, contributing to improved SCC resistance.

4. Compositional redistribution of alloying elements—Cu enrichment at grain boundaries and Zn enrichment within the matrix—combined with Zr-induced boundary stabilization,

reduced the electrochemical potential difference between the grain boundary and matrix. This dual mechanism accounts for the superior balance of strength and corrosion resistance achieved in the RRA-treated Zr-modified 7055 alloy.

Acknowledgment

This research was conducted with the support of the Advanced Materials and New Technology Department labs. It was funded by the Iranian Research Organization for Science and Technology (IROST), Tehran, Iran, fund No. 1012092001. I also acknowledge the contributions of all lab assistants for their diligent efforts in data collection.

Conflict of interest

The authors declare no conflicts of interest regarding this manuscript.

References

[1] Wei, L., Wei, P., Zhang, Z., Hu, L., Hu, Z., & Hua, L. (2025). Size Effects of Second-Phase Particles on the Ductile Behavior in 7075 Aluminum Alloy: Lattice Rotation and Coordination Deformation. *Journal of Alloys and Compounds*, 1039, 183266. https://doi.org/10.1016/j.jallcom.2025.183266

[2] Warner, T. (2006). Recently-Developed Aluminium Solutions for Aerospace Applications. *Materials Science Forum, 519-521*, 1271-1278. https://doi.org/10.4028/www.scientific.net/MSF.519-521.1271

[3] Chen, S., Chen, K., Peng, G., Jia, L., & Dong, P. (2012). Effect of Heat Treatment on Strength, Exfoliation Corrosion, and Electrochemical Behavior of 7085 Aluminum Alloy. *Materials & Design*, *35*, 93-98. https://doi.org/10.1016/j.matdes.2011.09.033

[4] Kim, G. Y., Kim, K. S., Kim, S. K., Yoon, Y. O., Cho, K. S., & Lee, K. A. (2013). High Cycle Fatigue Behavior of Eco7075-T73 Aluminum Alloy. *Advanced Materials Research, 690-693*, 1775-1778. https://doi.org/10.4028/www.scientific.net/amr.690-693.1775

[5] He, B., Wu, X., Liao, B., Yang, Y., Tang, S., Zhu, Q., Xiong, Y., Jia, Z., Meng, Y., & Cao, L. (2026). Revisiting the Evolution of Strength and Microstructure of Aluminum Alloy 7055 during Continuous Retrogression and Re-Ageing Treatment. *Journal of Materials Science & Technology, 256*, 42-52. https://doi.org/10.1016/j.jmst.2025.08.037

[6] Su, C. H., Chen, T. C., & Tsay, L. W. (2023). Improved Fatigue Strength of Cr-Electroplated 7075-T6 Al Alloy by Micro-Shot Peening. *International Journal of Fatigue*, *167*(part B), 107354. https://doi.org/10.1016/j.ijfatigue.2022.107354

[7] Palacios-Robledo, D., Fresneda-García, J., Lorenzo-Bonet, E., Guerra-Fuentes, L., Deaquino-Lara, R., Hernández-Rodríguez, M. A. L., & García-Sánchez, E. (2021). Tribological Analysis in Al–Mg–Zn Alloy Casting Processed through Equal Channel Angular Pressing, Compared with Al-7075 T6 Alloy. *Wear*, *476*, 203680. https://doi.org/10.1016/j.wear.2021.203680

[8] Zhang, J. C., Ding, D. Y., Zhang, W. L. Kang, S. H., Xu, X. L., Gao, Y. J., Chen, G. Z., Chen, W. G., & You, Z. H. (2014). Effect of Zr Addition on Microstructure and Properties of Al–Mn–Si–Zn-Based Alloy. *Transactions of Nonferrous Metals Society of China*, *24*(12), 3872-3878. https://doi.org/10.1016/S1003-6326(14)63545-7

[9] Liu, S. D., Chai, W. R., Wang, Q., Pan, Q. L., Li, A. D., Deng, Y. L., & Zhang, X. M. (2017). *Effect of Zr addition on localized corrosion behavior of Al–Zn–Mg alloy*. In *High Performance Structural Materials*, Chinese Materials Conference, pp. 247-254, Springer Singapore. https://doi.org/10.1007/978-981-13-0104-9_26

[10] Zhao, H., Ye, L., Cheng, Q., Kang, Y., & Zhang, W. (2023). Enhanced Mechanical Properties and Corrosion Resistance of 7055 Aluminum Alloy through Variable-Rate Non-Isothermal Aging. *Journal of Alloys and Compounds*, *943*, 169198. https://doi.org/10.1016/j.jallcom.2023.169198

[11] Zhu, M. Z., Xu, Y. X., Fang, H. C., Zhang, Q. Q., Zhang, Z., Chen, K. H., Hai-lin Yang , H. L., & Zhu, K. (2025). Effects of Yb/Zr Micro-Alloying on Microstructure, Mechanical Properties, and Corrosion Resistance of Al-Zn-Mg-Cu Alloy. *Journal of Central South University*, *32*(6), 1995-2008. https://journal.hep.com.cn/jocsu/EN/10.1007/s11771-025-5948-9

[12] Ren, J., Wang, R., Peng, C., Zhang, H., Xu, C., Wu, Y., & Feng, Y. (2020). Effect of Repetitious Retrogression and Re-Aging Treatment on the Microstructure, Strength, and Corrosion Behavior of Powder Hot-Extruded 7055 Al Alloy. *Materials Characterization*, *162*, 110190. https://doi.org/10.1016/j.matchar.2020.110190

[13] Jiang, H., Xing, H., Xu, Z., Yang, B., Liang, E., Zhang, J., & Sun, B. (2023). Effect of Zn Content and Sc, Zr Addition on Microstructure and Mechanical Properties of Al-Zn-Mg-Cu Alloys. *Journal of Alloys and Compounds*, *947*, 169246.

https://doi.org/10.1016/j.jallcom.2023.169246

[14] Liu, J., Shi, L., Su, R., Liu, T., & Li, G. (2025). Effect of Deep Cryogenic Treatment on Microstructure and Properties of Al-Cu-Mg-Ag Alloy with RRA. *Journal of Alloys and Compounds*, *1020*, 179574. https://doi.org/10.1016/j.jallcom.2025.179574

[15] Rodinger, T., & Ćorić, D. (2025). Retrogression and Re-Aging of 7xxx Series Aluminum Alloys: A Review of Microstructural Changes and Their Influence on Mechanical Properties and Corrosion Resistance. *Materials Today Communications, 49*, 114456. https://doi.org/10.1016/j.mtcomm.2025.114456

[16] ASTM International. (2016). *ASTM E8/E8M-16a: Standard Test Methods for Tension Testing of Metallic Materials*. ASTM International. https://store.astm.org/e0008_e0008m-16.html

[17] Shakouri, M., Esmailian, M., & Shabestari, S. (2018). Effect of Silver Addition on Mechanical Properties and Stress Corrosion Cracking in a Predeformed and Overaged 7055 Aluminum Alloy. *Journal of Testing and Evaluation*, *46*(5), 1891-1900. https://doi.org/10.1520/JTE20170137

[18] Shifler, D. A., & Enos, D. G. (2022). Marine corrosion testing. In Shifler, D. A. (Eds.), *LaQue's Handbook of Marine Corrosion* (pp. 379-420). John Wiley & Sons, Inc. https://doi.org/10.1002/9781119788867.ch15

[19] Torres, P. D. (2015). *Stress Corrosion Evaluation of Various Metallic Materials for the International Space Station Water Recycling System* (No. NASA/TM-2015-218206). NASA. https://ntrs.nasa.gov/citations/20150006942

[20] Marlaud, T., Deschamps, A., Bley, F., Lefebvre, W., & Baroux, B. (2010). Influence of Alloy Composition and Heat Treatment on Precipitate Composition in Al–Zn–Mg–Cu Alloys. *Acta Materialia*, *58*(1), 248-260. https://doi.org/10.1016/j.actamat.2009.09.003

[21] Bakker, H., Bonzel, H. P., Bruff, C. M., Dayananda, M. A., Gust, W., Horvath, J., Kaur, I., Kidson, G. V., LeClaire, A. D., Mehrer, H., Murch, G. E., Neumann, G., Stolica, N., & Stolwijk, N. A. (1990). In H. Mehrer (Eds.), *Diffusion in Solid Metals and Alloys*. vol. 26, Berlin, Springer. https://doi.org/10.1007/b37801

[22] Young, G. A., Jr., & Scully, J. R. (2002). The Effects of Test Temperature, Temper, and Alloyed Copper on the Hydrogen-Controlled Crack Growth Rate of an Al-Zn-Mg-(Cu) Alloy. *Metallurgical and Materials Transactions A*, *33*(4), 1167-1181. https://doi.org/10.1007/s11661-002-0218-y

[23] Wu, L. M., Seyring, M., Rettenmayr, M., & Wang, W. H. (2010). Characterization of Precipitate Evolution in an Artificially Aged Al–Zn–Mg–Sc–Zr Alloy. *Materials Science and Engineering: A*, *527*(4-5), 1068-1073. https://doi.org/10.1016/j.msea.2009.09.023

[24] Mukhopadhyay, A. K., Yang, Q. B., & Singh, S. R. (1994). The influence of zirconium on the early stages of aging of a ternary Al–Zn–Mg alloy. *Acta Metallurgica et Materialia*, *42*(9), 3083-3091. https://doi.org/10.1016/0956-7151(94)90406-5

Additional information

Correspondence and requests for materials should be addressed to M. Esmailian.

HOW TO CITE THIS ARTICLE

Shakoory, M.; Esmailian, M.; Taheri, M. (2025). Effect of Zr particles and RRA heat treatment on properties and grain boundary precipitation of 7055 Aluminum alloys, *J. Part. Sci. Technol. 11 (2) 93-100.*

DOI: 10.22104/jpst.2026.7865.1287
URL: https://jpst.irost.ir/article_1644.html